International Journal of Modern Manufacturing Technologies
ISSN 2067–3604, Vol. XII, No. 1 / 2020

APPLICATION OF ARTIFICIAL NEURAL NETWORKS FOR THE PREDICTION OF TOOL WEAR DURING TURNING OF HARDENED STEEL

Paweł Twardowski[1], Izabela Rojek[2], Natalia Znojkiewicz[1]

[1]Poznan University of Technology, Institute of Mechanical Technology, M. Skłodowskiej-Curie 3, 60-965 Poznań, Poland
[2] Kazimierz Wielki University, Institute of Computer Science, Chodkiewicza 30, 85-064 Bydgoszcz, Poland

Corresponding author: Izabela Rojek, izarojek@ukw.edu.pl

Abstract: The real-time wear of evaluation tools occurs for many reasons. The cutting process monitoring system is a tool that allows catastrophic tool wear to be eliminated. Based on multisensor systems, methods are created based on multiple monitoring models. In addition, the rapid development of artificial intelligence (AI) allows for the more effective application of these methods to predict the state of tool wear. In the presented work, the first stage of research concerns the application of neural networks to the possibility of predicting tool wear condition based on various input data such as: cutting forces, acoustic emission and mechanical vibrations. The second stage of the research concerns the development of models for the classification of the cutting edge's acceptability status, and a blunt cutting edge providing an example of mechanical vibrations. Measurements of selected physical quantities were carried out during the turning of hardened steel with constant cutting parameters.

Key words: artificial neural networks, effectiveness, diagnostic measures, prediction, classification, tool condition keywords.

1. INTRODUCTION

Nowadays, many methods are used that allow tool wear to be evaluated in real-time. The cutting process monitoring system is a tool that allows catastrophic tool wear to be eliminated. One of the newer methods used to monitor the condition of tool wear is the empirical method of EMD (Empirical Mode Decomposition), which is based on the decomposition of signals in the time domain. It was included in the paper (Shi et al., 2018), where it was used in the detection of the cracking of the tool based on the measurement of cutting forces. In addition, various algorithms are created which, using video systems, allow tool wear analysis to be performed (Zhang and Zhang, 2013). Large use in machining also allows indirect monitoring of tool wear based on cutting forces, the evaluation of chip morphology, mechanical vibrations and acoustic emission. In the work (Olufayo and Abou-El-Hossein, 2015), acoustic emission signals were used to diagnose ceramic inserts during milling at high speed cutting, where a multi-sensor system for classifying the wear of the tool in use was also used. Very often, cutting forces (Liu and Jolley, 2015; Wang et al., 2013) are used to diagnose the condition of the tool, and neural networks (Felusiak and Twardowski, 2018) are used for diagnostic inference. In addition to neural networks, wavelet transformation and spectral grouping algorithms are also used for diagnostic inference (Aghazadeh, 2018). An extensive overview of the applied wedge monitoring methods can be found in (Zhou and Xue, 2018). Many publications confirm that machining forces are the most sensitive to changes in tool wear. However, their industrial application involves constructional intervention of machine tools or causes restrictions in the working space. These limits are not only related to vibration and acoustic emission sensors that are easy to assemble and do not interfere with the design of the machine tools. Therefore, diagnostic methods based on vibration measurement and acoustic emissions are constantly being developed. One of the newer solutions is the use of multisensors due to the fact that different sensors are more correlated with subsequent stages of tool wear. This solution gives a full picture of the potential wear. After receiving the raw signals, signal processing and feature extraction methods are used, i.e. time domain analysis using autoregressive AR models, moving average MA models or ARMA mixed models, methods based on frequency domain analysis, wavelet transformation and the EMD empirical method. Based on multisensor systems, methods are being created based on multiple monitoring models (Das et al., 2018). In addition, the rapid development of artificial intelligence (AI) and advanced methods of inference allow for the more effective application of these methods to predict the state of tool wear (Khorasani and Yazadi, 2017; Kong et al., 2017; Savkovic et al., 2017; Varol and Ozsahin, 2017; Zhu and Liu, 2018).
The presented work concerns the application of artificial neural networks to the possibility of predicting the tool wear condition based on various

input data such as: cutting forces, acoustic emission, and mechanical vibrations. Measurements of selected physical quantities were carried out during the turning of hardened steel with constant cutting parameters.

2. EXPERIMENTAL SET-UP

The tests were carried out during the turning of 100Cr6 (61 HRC) hardened steel. The tool material was MC2 oxide ceramics (Al2O3+TiN), in the form of mechanically fastened inserts (SNGN120408). The tests were carried out on a TUR560E lathe with constant turning parameters: cutting speed v_c=180m/min, feed f= 0.08mm/rev and cutting depth a_p= 0.1mm.
After each pass (length of the shaft L= 150mm) the flank wear VB_c (the width of the flank wear on the tool cutting edge) was measured by means of a workshop microscope with a resolution of 0.01mm.
During turning, the values of the forces, (F_c(F_x), F_f(F_y) and F_p(F_z)), the acceleration of the vibrations in three directions (A_c(A_x), A_f (A_y) and A_p(A_z)) and the acoustic emission (by the broadband sensor and a 150 kHz resonance sensor) were measured. Figure 1 presents a simplified diagram of the measurement path, which takes into account the location of the sensors and additional components necessary for signal processing and analysis. Measurement of the forces, vibrations and acoustic emission was based on sensors using the piezoelectric effect.

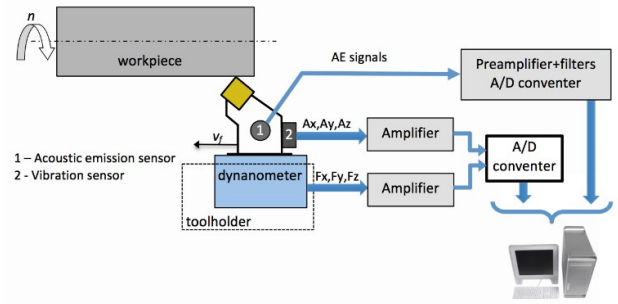

Fig. 1. Diagram of the measuring set-up used during the turning of hardened steel

To measure the components of the cutting forces, a piezoelectric sensor was used, which was placed on the lathe slide. As a diagnostic measure, the maximum, minimum and mean square values were selected. The vibration was measured using a three-component piezoelectric vibration acceleration sensor.
Digital signals were sent to the computer on the basis of which the mean square RMS values were determined for the tested quantities - equation (1):
The time intervals for which RMS values were determined were 4s and the obtained measures have been correlated with the corresponding tool wear values.

$$M_{RMS} = \sqrt{\frac{1}{T_2 - T_1}\int_{T_1}^{T_2}[x(t)]^2\,dt} \qquad (1)$$

Where: M_{RMS} - mean square value for any diagnostic measure.

15 repetitions were performed, i.e. under the same conditions, the wear process was carried out for 15 tool cutting edges. For each cutting edge, the testing was continued until the wear value VB_c≈ 0.4mm was reached. The following blunt criterion has been adopted: $\boldsymbol{VB_c}$**= 0.3mm**.

3. RESULTS AND DISCUSSION

3.1 Influence of tool wear on diagnostic measures

Figure 2 shows the relationship between the tool wear indicator VB_c and the cutting time t_s for all 15 cutting edges. To determine the dependence, the type of function was selected: $\boldsymbol{VB_c}$= $a\boldsymbol{t_s}^3$+$b\boldsymbol{t_s}^2$+$c\boldsymbol{t_s}$, 3rd degree polynomial, as the most representative for the tool wear process. This function reflects in the best way, the results obtained, and the coefficient R^2= 0.98, which indicates a high fitting to the selected mathematical function.

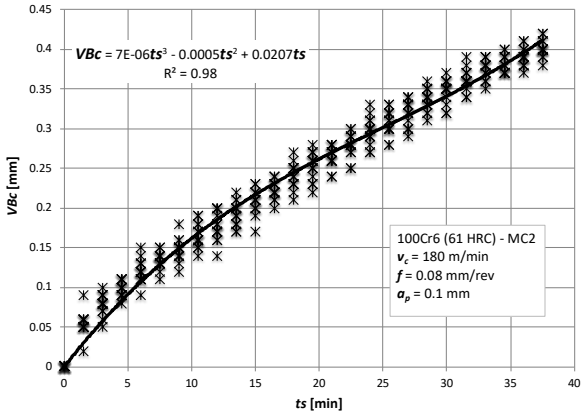

Fig. 2. Tool wear VB_c as a function of time t_s including all tests carried out

From the graph, it can be seen that the assumed dulling criterion VB_c= 0.3mm is reached for t_s≈25min. This criterion was selected on the basis of previous experience related to the machining of hardened steels. Above this value, the probability of chipping of the ceramic cutters increases significantly, due to, among others, an increase in the level of vibration amplitudes.
The next step was to recognise the relationship between tool wear and designated measures of diagnostic signals. Figure 3 shows an example of the dependence of the maximum F_p value as a function of tool wear VB_c. This dependence is described by the

linear function $\boldsymbol{F_{p\_max}}$= a$\boldsymbol{VB_c}$+b and the coefficient R^2=0.8. For all other diagnostic measures (i.e. F_{i_max}, F_{i_min}, F_{i_RMS}), the best results were also obtained for the linear function.

The relationship between vibration and acoustic emission in the function of tool wear looks different (Figures 4 and 5). In these cases, the exponential function was chosen to assess the correlation of vibrations and acoustic emission with the tool wear, for which R^2 was the largest.

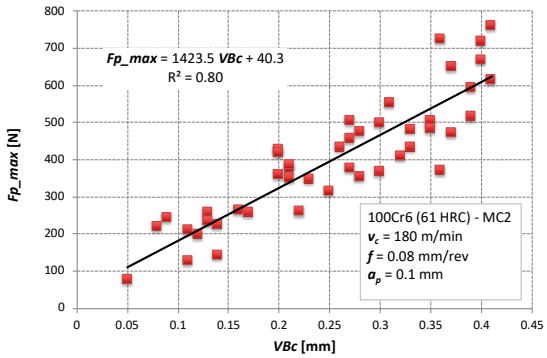

Fig. 3. Resistance component F_{p_max} in the function of tool wear VB_c

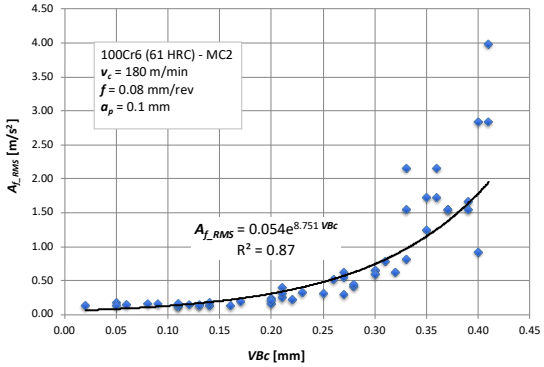

Fig. 4. Vibrations in the feed direction A_{f_RMS} as a function of tool wear VB_c

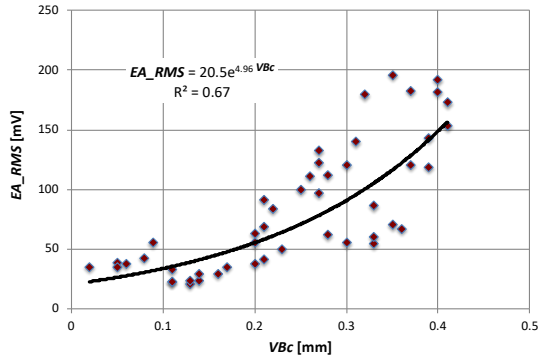

Fig. 5. Acoustic emission *EA_RMS* as a function of tool wear VB_c

Figures 4 and 5 show only examples of measures, and ultimately analysed:

cutting forces

- F_{p_min} – minimum value of thrust force,
- F_{p_max} – maximum value of thrust force,
- F_{f_min} – minimum value of feed force,
- F_{f_max} – maximum value of feed force,
- F_{c_min} - minimum value of cutting force,
- F_{c_max} – maximum value of cutting force.

vibration

- *af* 0-10kHz - RMS value of vibrations in the feed direction in the 0 - 10kHz band,
- *af* 0-2kHz - RMS value of vibrations in the feed direction in the 0 - 2kHz band,
- *af* 2-4kHz - RMS value of vibrations in the feed direction in the 2 - 4kHz band,
- *af* 5-8kHz - RMS value of vibrations in the feed direction in the 5 - 8kHz band,
- *ap* 0-10kHz - RMS value of vibrations in the thrust direction in the 0 - 10kHz band,
- *ap* 0-2kHz - RMS value of vibrations in the thrust direction in the 0 - 2kHz band,
- *ap* 2-4kHz - RMS value of vibrations in the thrust direction in the 2 - 4kHz band,
- *ap* 5-8kHz - RMS value of vibrations in the thrust direction in the 5 - 8kHz band.

acoustic emission

- *k1* 10-100kHz, - RMS value for the broadband sensor in the 10 - 100kHz band,
- *k1* 100-200kHz - RMS value for the broadband sensor in the 100 - 200kHz band,
- *k1* 10-500kHz - RMS value for the broadband sensor in the 10 - 500kHz band,
- *k1* k - RMS value for the broadband sensor in the 10 - 1000kHz band,
- *k2* 10-100kHz - RMS value for the resonance sensor in the 10 - 100kHz band,
- *k2* 100-200kHz - RMS value for the resonance sensor in the 100 - 200kHz band,
- *k2* 10-500kHz - RMS value for the resonance sensor in the 10 - 500kHz band,
- *k2* k - RMS value for the resonance sensor in the 10 - 1000kHz band.

3.2 Diagnostic inference

The main purpose of diagnostics of the tool's condition is to determine its degree of wear based on the measured physical quantities. At the same time, a different approach to this issue can be applied. In industrial practice, the determination of two states, being acceptable and unacceptable (i.e. that the tool should be replaced with a new one), is usually applied. For this purpose, a permissible tool wear value must be defined - the dullness criterion. In this work, the following relations have been adopted: VB_c <0.3mm – acceptable tool condition, VB_c ≥0.3mm - blunt tool. Figures 6 and 7 show the two distinct tool conditions

discussed for two exemplary force measures. The separation of the two areas, i.e. "acceptable tool condition" and "a blunt tool", is the task of a monitoring system working on the basis of various mathematical algorithms.

However, a two-step evaluation of the tool condition is not always sufficient. Often, the point is to evaluate what the condition of the tool will be in the next cycle, and if necessary, withdraw it before exceeding the allowable wear limit. In this situation, we are dealing with prediction. A valid mathematical model for prediction is used to assess the state of the tool at any time. The simplest model is the one-variable regression equation shown, for example, in Figures 8 and 9.

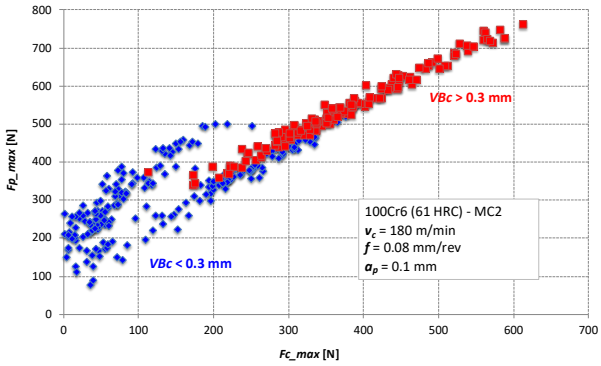

Fig. 6. Two tool conditions for F_{p_max} and F_{c_max}

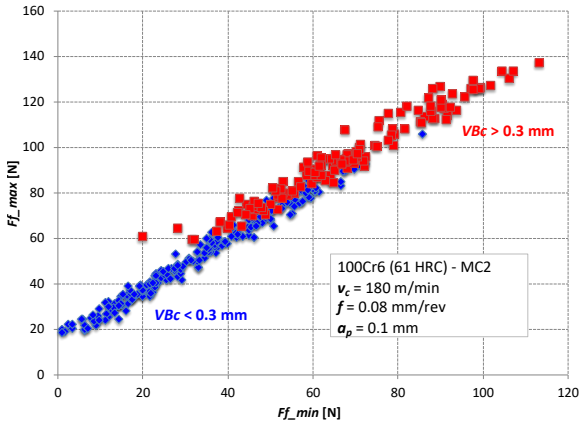

Fig. 7. Two tool conditions for F_{f_max} and F_{f_min}

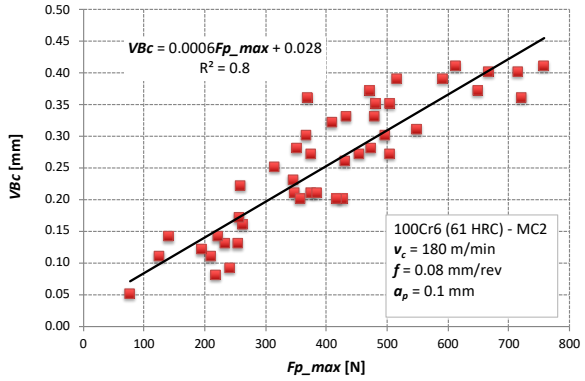

Fig. 8. An example of a one-variable model for F_{p_max} type: $y = a{\cdot}x + b$

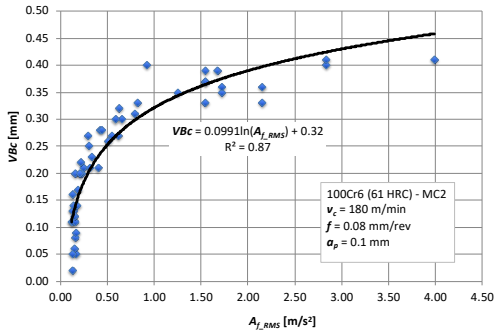

Fig. 9. An example of a one-variable model for A_{f_RMS} type: $y = a{\cdot}\ln(x) + b$

In the case of force components, a linear relationship of the type: $y = ax + b$, or $\boldsymbol{VB_c}$= a$\boldsymbol{F_i}$+b, is best suited for assessing tool wear. In such a situation, it is enough to substitute the appropriate value of the force component and read the value of the wear indicator. The same applies to measurements based on vibration signals or acoustic emission. The only difference is that in this case, the best suited dependence is the logarithmic function of the type: $y = a{\cdot}\ln(x)+b$, i.e. $\boldsymbol{VB_c}$= a·ln($\boldsymbol{A_i}$)+b, or $\boldsymbol{VB_c}$=a·ln ($\boldsymbol{EA_i}$)+b.

A one-variable regression model has the basic disadvantage of being imprecise. The natural dispersion of experimental results means that the predicted values are not precise and are sometimes characterised by a large error. Therefore, it is better to use multi-variable models or artificial intelligence algorithms, such as, neural networks.

3.3 Neural networks to evaluate the effectiveness of various diagnostic measures of cutting-edge status

At the stage of data preparation, the individual parameters used for the assessment were defined. Using the reinforced trees method, the importance (rank) of individual parameters was determined. This validity was examined for selected measures: cutting forces, vibrations, acoustic emission and all measures together. Figure 10 shows the charts of the importance of the individual parameters for individual measures. The maximum validity is 1.

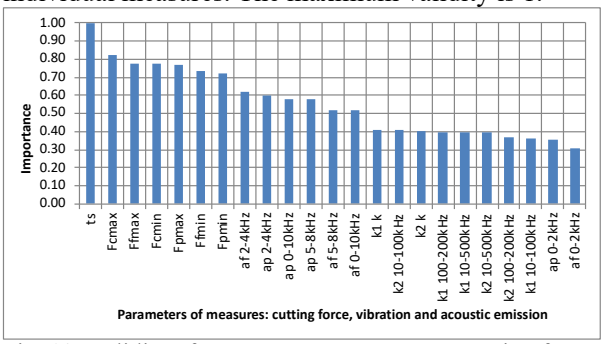

Fig. 10. Validity of measurement parameters: cutting force, vibration and acoustic emission

For the purpose of creating models of neural networks, the input parameters were normalised and coded. This was dictated by the diversity of ranges of individual parameters, and in the case of some artificial intelligence methods (e.g. neural networks), such range differences would cause the input data with a larger range to have an excessive effect on the results. In neural networks, the functions of neuron transition do not specify requirements as to the range of input values, and they generate output values belonging to a strictly defined range. At the boundaries of this range in the neuron characteristic, there is a "saturation" effect, which means that in fact, the input values should also belong to a limited range. The limited range of possible network responses in connection with the requirement to use only data in numerical form requires the use of a pre-processing step before input to the network input (preprocessing the input data) and the process of transforming and interpreting the output data received from the network (postprocessing the results) (Tadeusiewicz et al., 2014).

There are many options to perform the mentioned transformations of input and output data: for example, the external numerical values can be scaled to a range suitable for the network. In typical cases, the raw data is scaled in a linear manner. In these studies, min-max normalisation was applied. It is based on checking how much the field value is greater than the minimum value (X), and then scaling this difference by the range - equation (2):

$$X^* = \frac{X - \min(x)}{\max(X) - \min(X)} \tag{2}$$

Data coding

The second categories of data are nominal data, which may be two- or multi-state, e.g. the tool cutting edge condition parameter has two states: an acceptable cutting edge, a blunt cutting edge. In the first stage of the research, one-of-N coding was chosen, which consists of using several numerical variables in the network structure instead of one nominal one. For example, for the wedge state parameter, the number of numeric variables is 2 and is equal to the number of possible values of the nominal variable: good wedge = {1,0}, blunted wedge = {0,1}. With such data coding, the number of network inputs and outputs increases.

VB_c tool wear detection was performed on the basis of the following measurements: cutting forces, vibrations and acoustic emission. Separate models of artificial neural networks were created for individual measures and for all together. Next, the results of the neural networks were compared to the actual values measured during the machining process.

Multi-layer neural networks with backward error propagation (MLP) were used to build the models.

3.4 Prediction of tool condition using neural networks for measures: cutting force, vibrations, acoustic emission

Neural networks are a very good tool for forecasting and classification (Rojek, 2010, 2017).

In order to obtain the most effective neural network models, the evaluation of the cutting edge was parameterised with different sizes. Table 1 shows the inputs and outputs of the neural networks for individual measures.

The neural network model created on the basis of the measure of:

–cutting forces had 7 inputs (t_s, F_{p_min}, F_{p_max}, F_{f_min}, F_{f_max}, F_{c_min} and F_{c_max}) and 1 output (VB_c),

–vibration had 9 inputs (ts, af 0-10kHz, af 0-2kHz, af 2-4kHz, af 5-8kHz, ap 0-10kHz, ap 0-2kHz, ap 2-4kHz and ap 5-8kHz) and 1 output (VB_c),

–acoustic emission had 9 inputs (ts, k1 10-100kHz, k1 100-200kHz, k1 10-500kHz, k1 k, k2 10-100kHz, k2 100-200kHz, k2 10-500kHz and k2 k) and 1 output (VB_c),

–total had 23 inputs (t_s, F_{p_min}, F_{p_max}, F_{f_min}, F_{f_max}, F_{c_min}, F_{c_max},, af 0-10kHz, af 0-2kHz, af 2-4kHz, af 5-8kHz, ap 0-10kHz, ap 0-2kHz, ap 2-4kHz, ap 5-8kHz, k1 10-100kHz, k1 100-200kHz, k1 10-500kHz, k1 k, k2 10-100kHz, k2 100-200kHz, k2 10-500kHz and k2 k) and 1 output (VB_c).

Table 1. Inputs and outputs of neural networks MLP

Measures	Input parameters NN	Output parameter
Cutting forces	t_s, F_{p_min}, F_{p_max}, F_{f_min}, F_{f_max}, F_{c_min} and F_{c_max}	VB_c
Vibrations	ts, af 0-10kHz, af 0-2kHz, af 2-4kHz, af 5-8kHz, ap 0-10kHz, ap 0-2kHz, ap 2-4kHz and ap 5-8kHz	
Acoustic emission	ts, k1 10-100kHz, k1 100-200kHz, k1 10-500kHz, k1 k, k2 10-100kHz, k2 100-200kHz, k2 10-500kHz and k2 k	

Figure 11 shows structure of the MLP neural network on the basis of measurement of cutting forces.

The neural network models were built with one hidden layer, in which the number of neurons was changed experimentally (from 4 to 20). One of the most widely used learning algorithms, i.e. the BFGS algorithm (Broyden – Fletcher – Goldfarb - Shanno algorithm - MLP network learning algorithm) was used, in which the number of learning epochs was changed (from 10 to 150). The SOS function (error function in the form of the sum of squared differences) was used as the

error function - equation (3).

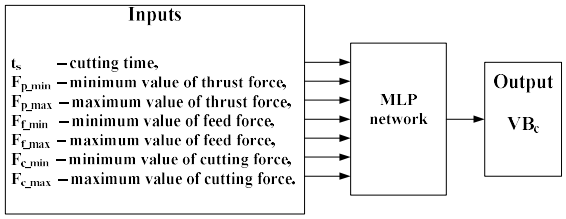

Fig. 11. Structure of MLP network on the basis of measurement of cutting forces

Figure 12 shows the values of the SOS error function for the selected MLP neural networks for the cutting force measure. In addition, the activation function was changed in the hidden and output layers (functions: Linear, Logistic, Exponential, Tanh, Softmax). Table 2 shows the best neural networks for the individual diagnostic measures.

$$E_{SOS} = \sum_{i=1}^{N} (y_i - t_i)^2 \qquad (3)$$

Where: N - number of examples (input / output pairs) used for learning, y_i - network prediction (network output), t_i - "real" value (output according to data) for the i^{th} case.

Fig. 12. SOS error function values for the selected MLP networks for the cutting force measure

Table 2. The best MLP network models for diagnostic measures

NS	E %	ER	BA	AH	AO	DM
7-8-1	99	0.000065	94	Tanh	Tanh	Cutting forces
9-11-1	99	0.000330	24	Tanh	Logistic	Vibrations
9-10-1	99	0.000087	67	Tanh	Logistic	Acoustic emission
23-19-1	99	0.000074	32	Logistic	Tanh	total

Where: NS - NN Structure, E - Effectiveness, ER – Error, BA - BFGS Algorithm, AH - Activation function in the hidden layer, AO - Activation function in the output layer, DM - Diagnostic measure

Worse efficiency results were obtained by networks with fewer neurons in the hidden layer (eg 4, 5), fewer learning epochs (eg 5, 20) or worse functions that were used as activation functions (e.g. linear).

The estimation of neural network models was made on the basis of the correlation coefficient. The closer the correlation coefficient approaches 1, the better the model. For example, for the best neural network (MLP 9-10-1) for acoustic emission, the correlation coefficient was determined by the values: learning - 0.992487, testing - 0.992186 and validation - 0.993731. However, for a slightly worse neural network (9-13-1), the correlation coefficient was as follows: learning - 0.964746, testing - 0.970827 and validation - 0.970501. Figure 12 presents R2 distribution graphs for the individual phases of creating a neural network model (learning, testing, validation) for acoustic emission for these two selected neural networks (MLP 9-10-1, MLP 9-13-1).

Figure 13 clearly shows that during training, all experimental and predicted values almost perfectly matched the regression line, i.e. R2 = 0.992487 for MLP 9-10-1. This means that the network has been satisfactorily trained. When testing and validating the network, several experimental values are located a little further from the regression line. Therefore, the R2 value becomes slightly less than 1 for the NN model.

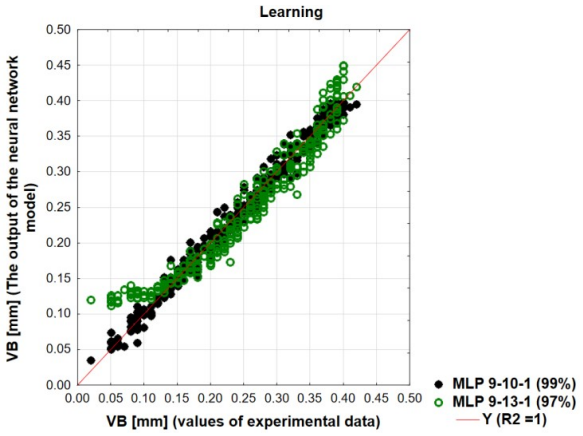

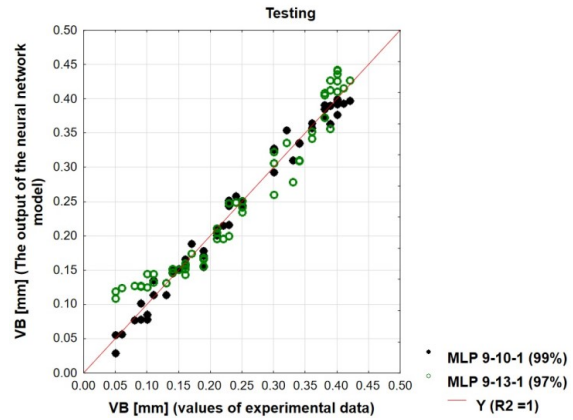

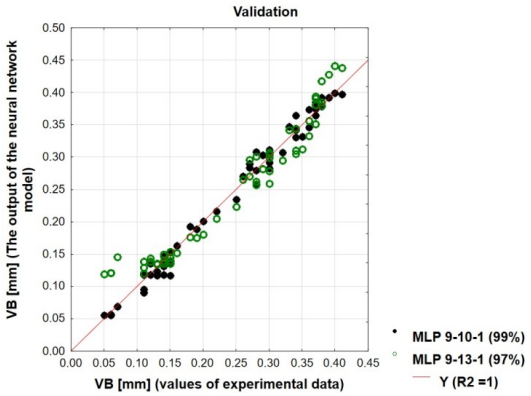

Fig. 13. Evaluation of neural network models using the correlation coefficient

The models of neural networks for new input data were also validated (Figure 14). Each time, 10 new real values were given to the input of the neural network. In response, the network reported results in the form of VB_c values. Figure 14 compares the responses of neural networks with the real ones obtained from the experiment.

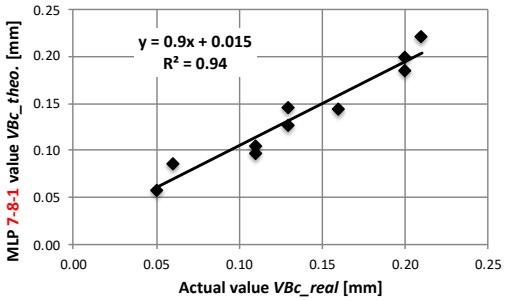

a)The result of the best network for cutting forces

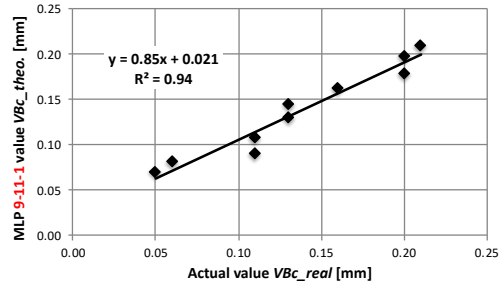

b)The result of the best network for vibrations

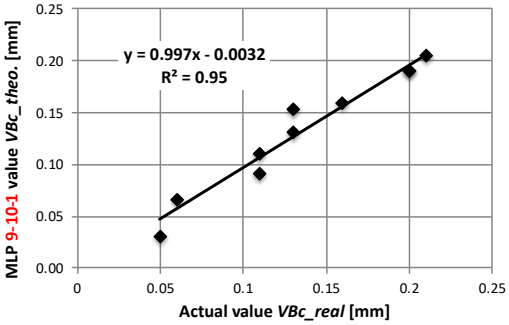

c)The result of the best network for acoustic emission

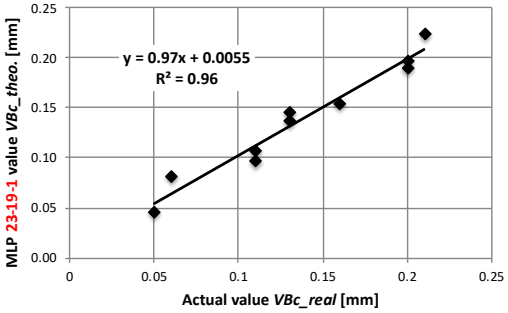

d)The result of the best network for all measures together

Fig. 14. Comparison of the operation of the best networks created for each diagnostic measure separately and together with the real values of VB_c obtained from the experiment

Figure 14 shows charts of the best models of neural networks for cutting forces, vibrations, acoustic emission and the graph, which was based on all measures together. All these neural networks have 99% efficiency. These networks have been parameterised with various parameters to achieve the same best performance. When comparing the operation of neural networks for 10 new values of measurements with the actual values from the process, it was found that the most-similar graph of the network is the grid plot for acoustic emission and cutting forces. In two points, we see slightly larger discrepancies (for measurements 3 and 6 for acoustic emission, and for measurements 2 and 6 for cutting forces), and for the remaining measurement points, the results are very similar. Additional real measurements could be made to diagnose the cause of such a result for the neural networks. The worst divergent results were provided by the neural network for vibrations.

3.5 Classification of wedge status using neural networks for vibrations

The second stage of the research concerned the development of models for the classification of the cutting edge's status as an acceptable or blunt cutting edge. This division results from the value of VB_c. In this case, nominal values appeared next to the numerical data (acceptable cutting edge and blunt cutting edge).

Neural network classification models are shown for the vibration measure. A training, testing and validation file was developed. Neural one-directional multilayer networks with backward error propagation (MLP) were also used to build classification models.

In order to obtain models of neural networks with the best effectiveness of classification of cutting edges as good or blunt, they were parameterised with different values.

The following values were given for the network

input: t_s, a_f 0-10kHz, a_f 0-2kHz, a_f 2-4kHz, a_f 5-8kHz, a_p 0-10kHz, a_p 0-2kHz, a_p 2-4kHz, a_f 5-8kHz and VB_c. At the output of the network was the nominal value: cutting edge_condition. So the network had 10 inputs and 1 output. Networks with one hidden layer were built, in which the number of neurons from 4 to 25 was changed. One of the most widely used learning algorithms was used, i.e. the BFGS algorithm (Broyden-Fletcher-Goldfarb-Shanno algorithm), in which the number of learning epochs was changed (from 4 to 30). The SOS function (error function in the form of sum of squares of differences) and mutual Entropy was used as the error function. The error functions in the form of sum squares were originally used to solve regression problems. They are also used for classification, however a real neural classifier should have a different error function - Cross Entropy, which has the following form - equation (4):

$$E_{CE} = -\sum_{i=1}^{N} t_i \ln\left(\frac{y_i}{t_i}\right) \tag{4}$$

It is assumed that the output variable is subjected to polynomial distribution, in contrast to the Sum of Squares, in which the output variable has a normal distribution.

In addition, the activation function was changed in the hidden and output layers (functions: Linear, Logistic, Exponential, Tanh, Softmax).

The most effective was the network with the structure 10-8-1 (98.14% effectiveness), in which the Tanh function was used as an activation function in the hidden layer, and the Softmax function in the initial, with 6 as the number of learning epochs. Worse results of effectiveness were provided by the networks with fewer neurons in the hidden layer (e.g. 5 neurons), fewer learning epochs (e.g. 4), or worse activation functions (e.g. linear). Table 3 presents the results of the 10-8-1 network classification. In 232 cases, the classification of the acceptable cutting edge was poorly classified 7 times, while in the case of the blunted cutting edge, only 1 was wrongly classified in a range of 143 cases.

Table 3. The results of the best network classification

Cases	Cutting edge condition-good	Cutting edge condition-blunt
Total	232	143
Correct	225	142
Incorrect	7	1
Correct (%)	96.98	99.30
Incorrect (%)	3.02	0.70

The neural network models were validated with new input data. Of the 20 new datasets given for the MLP 10-8-1 network entry, only one answer was wrong. Table 4 presents the comparison of the network response with the actual values from the experiment.

Table 4. Comparison of the network response with real values from the experiment

Input parameters for vibrations (af – feed direction, ap - thrust direction)										Cutting edge	
ts [min]	af [m/s^2] 0-10 kHz	af [m/s^2] 0-2 kHz	af [m/s^2] 2-4 kHz	af [m/s^2] 5-8 kHz	ap [m/s^2] 0-10 kHz	ap [m/s^2] 0-2 kHz	ap [m/s^2] 2-4 kHz	ap [m/s^2] 5-8 kHz	VBc [mm]	actual classification results	network responses MLP 10-8-1
13.50	0.2306	0.0700	0.0907	0.1953	0.2596	0.0577	0.0833	0.2364	0.20	good	good
15.00	0.2476	0.0717	0.0820	0.2169	0.2726	0.0552	0.0741	0.2535	0.21	good	good
16.50	0.3318	0.0684	0.1714	0.2558	0.3424	0.0589	0.1572	0.2901	0.23	good	good
18.00	0.3027	0.0740	0.1182	0.2587	0.3676	0.0876	0.1252	0.3221	0.25	good	good
19.50	0.2977	0.0692	0.0939	0.2676	0.3652	0.0771	0.1017	0.3331	0.27	good	good
21.00	0.4183	0.0738	0.1488	0.3705	0.4862	0.0721	0.1383	0.4502	0.28	good	good
22.50	0.6534	0.1091	0.1933	0.5897	0.7690	0.1110	0.1827	0.7207	0.30	**blunt**	**good**
24.00	2.6481	0.0882	0.1168	2.6186	3.1501	0.2602	0.2554	3.0943	0.33	blunt	blunt
25.50	0.9050	0.1068	0.1203	0.7419	1.0734	0.3523	0.1292	0.9536	0.33	blunt	blunt
27.00	0.8221	0.0970	0.2018	0.7390	0.7110	0.1902	0.1811	0.6254	0.33	blunt	blunt
28.50	1.2501	0.0918	0.1336	1.2281	0.8999	0.0725	0.1064	0.8852	0.35	blunt	blunt
30.00	2.1535	0.1695	0.1817	2.1032	1.8382	0.3952	0.1864	1.7637	0.36	blunt	blunt
31.50	0.6503	0.1019	0.1190	0.6208	0.8026	0.0790	0.1042	0.7852	0.37	blunt	blunt
33.00	1.5474	0.1020	0.1342	1.5268	1.8717	0.0828	0.1221	1.8597	0.39	blunt	blunt
34.50	0.8455	0.1076	0.1064	0.8241	0.7259	0.1529	0.1028	0.6926	0.40	blunt	blunt
36.00	3.9915	0.1776	0.1684	3.9752	4.7527	0.1161	0.1649	4.7391	0.41	blunt	blunt
37.50	2.8356	0.1640	0.1570	2.8217	3.8501	0.2054	0.2254	3.8284	0.41	blunt	blunt
1.50	0.3269	0.0824	0.0999	0.2524	0.3955	0.0995	0.1018	0.3233	0.02	good	good
3.00	0.1312	0.0725	0.0523	0.0931	0.1323	0.0570	0.0420	0.1093	0.05	good	good
4.50	0.1575	0.0681	0.0591	0.1254	0.1705	0.0561	0.0493	0.1507	0.08	good	good

3.6 The use of developed models in the turning hardened steel process monitoring application

The turning hardened steel process monitoring application uses both prediction and classification models. The prediction of tool condition is made by neural networks, which predict the tool wear indicator VBc on the base of measured cutting force, vibrations, and acoustic emission. Next, neural networks classify tools based on: blunt cutting edge vs. good cutting edge, and give information to the CNC machine operator. Figure 15 shows application screens. The main of application is shown in Figure 15(a). Figure 15(b) shows VBc forecasting by the neural network based on the measured cutting force, and Figure 15(c) shows the classification of the tool's state. After entering the data, the neural network is started and we get the neural network output.

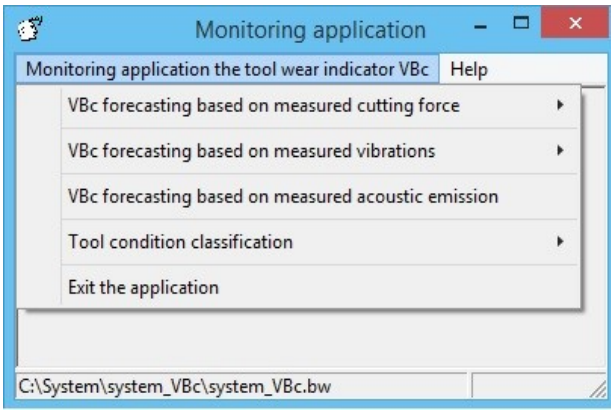

a) Application menu

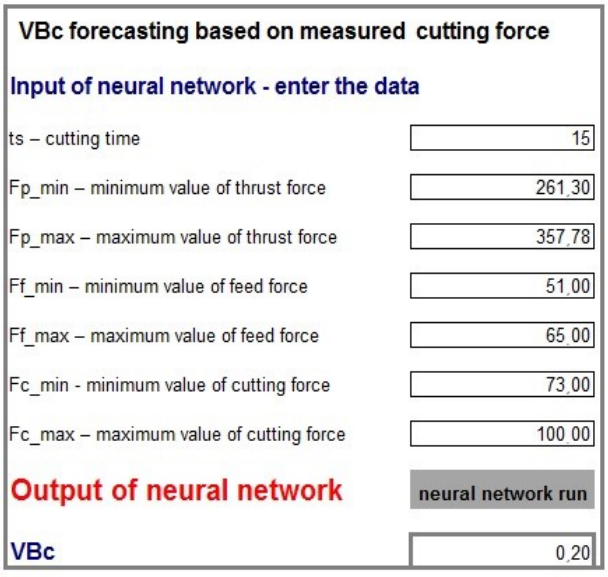

b) VBc forecasting by neural network

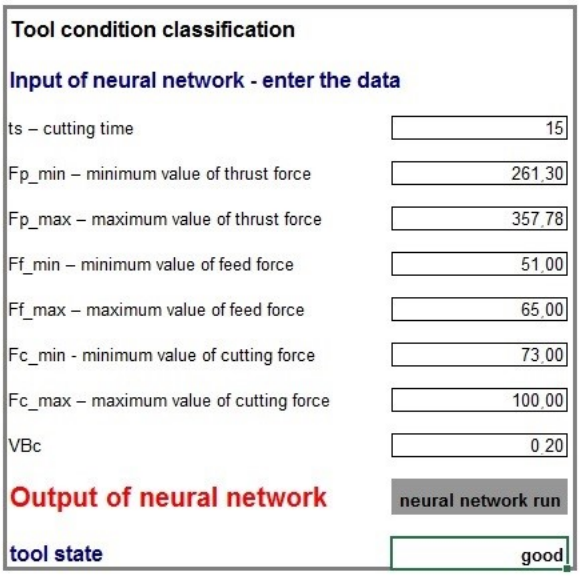

c) Classification of tool state

Fig. 15. Examples of application screens

4. CONCLUSIONS

The conducted research showed the usefulness of MLP neural networks to evaluate the effectiveness of various diagnostic measures in the classification and prediction of the condition of a tool cutting edge during the turning of hardened steel. The neural networks used provide excellent opportunities to use the data obtained from the machining process. The predictive neural networks used to evaluate the effectiveness of various diagnostic measures showed that the best results were obtained for the measure of cutting forces and acoustic emission. When selecting of cutting force sensors, the greater structural interference of the machine tools or the limitations related to the working space should be taken into account. Therefore, it seems better to use acoustic emission sensors that do not have such limitations. Neural networks confirmed the effectiveness of a diagnostic measure in the form of acoustic emission to assess the condition of the cutting edge. Neural networks cope very well with problems of grading a tool's condition as good and blunt. This is illustrated for the measure of vibration.

5. REFERENCES

1. Aghazadeh, F., Tahan, A., Thomas, M., (2018). *Tool Condition Monitoring Using Spectral Subtraction Algorithm and Artificial Intelligence Methods in Milling Process,* Int.J. Mech. Eng. Rob. Res., **7**(1), 30-34.

2. Das, P. P., Gupta, P., Das, S., Pradhan, B. B., Chakraborty, S., (2018). *Application of grey-fuzzy approach in parametric optimization of EDM process*

in machining of MDN 300 steel, Proceedings of 8th TSME-International Conference on Mechanical Engineering (TSME-ICoME 2017), **297**(012013), IOP Publishing, Bangkok.
3. Felusiak, A., Twardowski, P., (2018). *Diagnosis of edge condition based on force measurement during milling of composites*, Arch. Mech. Tech. Mater., **38**, 8-14.
4. Khorasani, A., Yazdi, M.R.S., (2017). *Development of a dynamic surface roughness monitoring system based on artificial neural networks (ANN) in milling operation,* Int.J. Adv. Manuf. Technol., **93**(1-4), 141–151.
5. Kong, D., Chen, Y., Li, N., (2017). *Hidden semi-Markov model-based method for tool wear estimation in milling process*, Int.J. Adv. Manuf. Technol., **92**(9–12), 3647–3657.
6. Liu, T., Jolley, B., (2015). *Tool condition monitoring (TCM) using neural networks*, Int.J. Adv. Manuf. Technol., **78**(9-12), 1999–2007.
7. Olufayo, O., Abou-El-Hossein, K., (2015). *Tool life estimation based on acoustic emission monitoring in end-milling of H13 mould-steel*, Int.J. Adv. Manuf. Technol., **81**(1-4), 39–51.
8. Rojek, I. (2010). *Hybrid neural networks as prediction models*, Lecture Notes in Artificial Intelligence, LNAI 6114**,** part II, Rutkowski, L., Scherer, R., Tadeusiewicz, R., Zadeh, L.A., Zurada, J.M. (Eds), pp. 88 – 95, **(**Berlin, Heidelberg: Springer-Verlag**)**.
9. Rojek, I. (2017). *Technological Process Planning by the Use of Neural Networks,* J. Artificial Intelligence for Engineering Design, Analysis and Manufacturing AI EDAM, **31**(1), 1-15.
10. Savkovic, B., Kovac, P., Mankova, I., Gostimirovic, M., Rokosz, K., Rodic, D., (2017). *Surface roughness modeling of semi solid aluminum milling by fuzzy logic*, J. of Advances in Technology and Engineering Studies, **3**(2), 34-46.
11. Shi, X., Wang, X., Jiao, L., Wang, Z., Yan, P., Gao, S., (2018). *A real-time tool failure monitoring system based on cutting force analysis*, Int.J. Adv. Manuf. Technol., **95**(5-8), 2567–2583.
12. Tadeusiewicz, R., Chaki, R., Chaki, N., (2014). Exploring Neural Networks with C#, *(*Boca Raton: CRC Press Taylor & Francis Group).
13. Wang, G., Guo, Z., Yang, Y., (2013). *Force sensor based online tool wear monitoring using distributed Gaussian ARTMAP network*, Sensors Actuators A: Physical, **192**, 111–118.
14. Varol, T., Ozsahin, S., (2017). *Artificial neural network analysis of the effect of matrix size and milling time on the properties of flake Al-Cu-Mg alloy particles synthesized by ball milling,* Particulate Science and Technology, **37**(3), 381-390.
15. Zhang, C., Zhang, J., (2013). *On-line tool wear measurement for ball-end milling cutter based on machine vision*, Computers in Industry, **64**, 708–719.
16. Zhou, Y., Xue, W., (2018). *Review of tool condition monitoring methods in milling processes*, Int.J. Adv. Manuf. Technol., **96**(5-8), 2509–2523.
17. Zhu, K., Liu, T., (2018). *Online Tool Wear Monitoring Via Hidden Semi-Markov Model With Dependent Durations,* IEEE Transactions on Industrial Informatics, **14**(1), 69-78.

Received: March 14, 2020 / Accepted: June 15, 2020 / Paper available online: June 20, 2020